

Catalytic degradation of methyl orange using biogenic nanosilver and its phytotoxicity evaluation

V Ramalingam¹, S Dhanasundari², P Nithiya² & R Rajaram*¹

¹DNA Barcoding and Marine Genomics lab, Department of Marine Science,
Bharathidasan University, Tiruchirappalli 620 024, Tamil Nadu, India

²Department of Biotechnology, Dhanalakshmi Srinivasan College of Arts and Science for Women,
Perambalur 621 212, Tamil Nadu, India

Email: drrajaram69@rediffmail.com; dnabarcodingram@gmail.com

Received 18 November 2015; accepted 5 October 2016

The cell free extract of *Staphylococcus aureus* has been used to reduce the 1mM silver nitrate into silver nanoparticles (AgNPs) in biological manner. The colour change from yellowish to brown colour is primary confirmation of AgNPs synthesis. Further, the synthesized AgNPs have been characterized by UV-vis for confirmation of reduction process. The morphology of AgNPs is visualized using transmission electron microscope (TEM), selected area electron diffraction (SAED), scanning electron microscope (SEM) is used to determine the size and zeta potential of AgNPs. The X-ray powder diffraction (XRD) is confirmed the presence of silver and its structure and the Fourier transform infrared spectroscopy (FT-IR) is used to determine the functional group that actively involved in methyl orange (MO) degradation. For application of AgNPs, different concentration (10-200 µg/mL) of AgNPs has been used to degrade the different concentration (100-2000 µg/mL) of MO. Roughly, 62% of MO (2000 µg/mL) has been degraded after treated with 200µg/mL of AgNPs. Further, the degradation is confirmed using FT-IR analysis that show the AgNPs break down the N=N bond of MO and dispersed it. The treated dye further evaluated its phytotoxicity against *Oryza sativa* and the results indicate that the treated dye has less toxicity than untreated.

Keywords: Silver nanoparticles, TEM, Methyl orange degradation, FT-IR, Phytotoxicity

Azo dyes are the major and flexible group of dyes that are xenobiotics, lethal and found to have revolt and solidity in environment, leads to the aesthetic and environment problems¹. Numerous commercial industries such as textile, plastic, pharmaceutical, leather, cosmetic, paper and food industries released the synthetic compounds and dyes². The production of inorganic compounds and their purpose for human interests is necessary but a severe and repulsive release into ambient environment is burden³. The existence of one or more azo bonds in azo dyes with aromatic rings makes aromatic nucleus that provides structurally diverse⁴ and prove to be toxic, mutagenic and carcinogenic⁵.

Today environmental protection has become more and more important for human beings, and some toxic and stable dye molecules like Methyl Orange (MO) are dangerous to the environment⁶. The technologies like UV radiation and hydrogen peroxide are not efficiently treating the colour dyes due to their chemical stability. Currently, photocatalytic degradation of dyes receives the attention owing to

the effective decolouration of dyes⁷. Degradation of dyes started with reducing the rift of azo group aromatic amines that leads to the mutagenic and carcinogenic effects on living organisms⁸.

Recently, metal nanoparticles were reported as effective photocatalysts for degrading chemical complexes, under ambient temperature with visible light illumination⁹. The advancement of organic impressed process for the synthesis of nanomaterials is developing into an extensive branch of nanotechnology¹⁰. In this modern technology, a great number of chemical and physical methods were applicable to synthesize various kind of metal nanoparticles but these are toxic, cost effective and instability¹¹. To rectify this problem, the green synthesis of metal nanoparticles have received more attention due to less toxic, stability, cheap and eco-friendly approach.

In the numerous account of metals, the researcher focuses on silver nanoparticles (AgNPs) owing to its wide range application in various fields such as anticancer agent, antifouling agent, antimicrobial agent, catalytic agent etc. The bacteria mediated

synthesis of AgNPs using *Bacillus licheniformis*¹², *B. megaterium*¹³, *Klebsiella pneumonia*¹⁴ and *Pseudomonas aeruginosa*¹⁵ have been reported. Nevertheless, the study and mechanism of AgNPs in photocatalytic degradation were limited. The present study aims to synthesize the AgNPs using culture supernatant of *S. aureus* for degradation of MO. The synthesized AgNPs were characterized by SEM, XRD and FT-IR. The degradation of MO was confirmed by UV-vis and FT-IR.

Experimental Section

Sample collection

The soil samples were collected from industrially contaminated sites from SIPCOT industrial complex, consists of various dye producing companies, Cuddalore coast (11°41'00" N; 79° 45' 40" E), Southeast Coast of India. The collected sediments were kept in icebox and transported to the laboratory in aseptic condition and air dried for one week and kept at 45°C for 1 h to minimize the bacterial contaminants.

Isolation of bacteria

From the collected samples, 1g was taken and diluted into an Erlenmeyer's flask containing 99 mL of sterile 50% seawater. The samples suspension was diluted up to 10⁻⁵ levels and 1mL of the diluted suspension was spread over the surface of nutrient agar medium prepared in 50% seawater to enhance the isolation of marine bacteria. The petri plates were incubated at 28 ± 2°C and the colonies were observed from 2nd day onwards. Strains of marine bacteria were picked out and purified by repeated streaking on nutrient agar plates¹⁶. The pure culture was identified using 16s rRNA amplification¹⁷ and the sequences were submitted to Genbank database (KF554244).

Synthesis of AgNPs

The isolated pure bacterial strain was sub-cultured in 100 mL of nutrient broth and incubated in shaker for 24 h at 160 rpm. After incubation, the culture was centrifuged at 10000 rpm for 10 min and the pellet was discarded. 5 mL of culture supernatant was added to 95 mL of 1 mM concentration of silver nitrate solution contained 250 mL conical flask. The conical flask was kept in shaker for 8 h¹⁵ and the colour change from yellowish to brown was analysed.

Characterization of nanoparticles

The synthesis of AgNPs was primarily confirmed by measuring the surface plasmon resonance using

UV-visible double beam spectrophotometer (UV-1800, Shimadzu, Japan). The morphology and presence of silver in nanomaterial was confirmed using a SEM equipped with Energy-dispersive X-ray spectroscopy (EDS) (Carl-Zeiss), TEM with SAED (JEOL 2100F) and XRD of AgNPs was obtained using powder XRD (PANalytical X'pert PRO) in 2θ range from 10°- 80°. The size and zeta potential of AgNPs was measured using DLS (Zetasizer-Nano-ZS90). FT-IR spectral analysis was carried out in the range of 4000-400 cm⁻¹ with a Spectrum RX-1 FT-IR spectrophotometer (JASCO 460 plus FT-IR) using KBr pellets. Using the XRD data, the AgNPs size was confirmed by Debye-Scherrer Equation.

Photocatalytic degradation of methyl orange

The photocatalytic activity of AgNPs was evaluated by measuring photocatalytic degradation of MO in water under the illumination of UV light. The experiment was carried out by dispersing the different concentration of photocatalyst (200 µg/mL) in different concentration of MO aqueous solution and magnetically stirred in dark. Subsequently, the suspension was irradiated with UV light. 2 mL samples were withdrawn from the above suspension at different time intervals and it was filtered through a syringe filter to completely remove the catalyst particles. The obtained samples were analyzed using UV-Vis spectroscopy by recording variations in absorbance at wavelength of 498 nm¹⁸.

FTIR analysis for dye degradation

Decolorized dye sample (10 mL) was taken after 24 h of incubation and centrifuged at 12000 rpm for 15 min, filtered through 0.45 µm membrane filter (millipore). The filtrate was extracted with diethyl ether and evaporated in rotary vacuum evaporator in temperature controlled water bath (60°C) and residue was used for FTIR analysis¹⁹ to find out the changes of functional groups as well as structure in MO (Fig. 1).

Consumption of MO by AgNPs

The MO consumed by AgNPs was quantified using the standard curve of MO equivalent (MOE) (µg/mL) using the equation based on the calibration curve: $y = 0.013x + 0.287$, $R^2 = 0.993$, where x was absorbance and the y was MOE µg/mL at final concentration of 2 mg/mL.

Phytotoxicity analysis

The phytotoxicity analysis of untreated and degraded dye evaluated its toxicity in the growth of *Oryza sativa*

(rice) by following the method of Shah *et al.*²⁰. The untreated and treated dye (2000 µg/mL) with AgNPs (200 µg/mL) was used for the phytotoxicity evaluation while the control was run by watering the seeds with distilled water. Choosing the high concentration of AgNPs, untreated and treated dye to evaluate the phytotoxicity will be more effective in the present than choosing the low concentration. Germination (%), shoot length, root length, phenols and flavonoids content was recorded after 15 days of treatment. The presence of phenols and flavonoids are expressed in microgram of galic acid and rutin respectively that equivalent of 1 g/mL of solvent extracts were achieved from the following linear relationships: f(concentration of galic acid/ rutin) = yield of phenols/flavonoids.

Results and Discussion

The green synthesis of metal nanoparticles has a foremost concentration of researchers in recent times owing to the endless application. The biological agents in the form of microbes are efficient candidates for the synthesis of nanoparticles that are economic, simpler to synthesize and the method is greener in approach. The present study, the

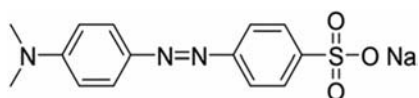


Fig. 1 — Structure of Methyl Orange

cell free extract of *S. aureus* was used to reduce the silver nitrate into nanoparticles by changing the colour from yellowish to brown which is evidence for synthesis of AgNPs. The colour change was observed after incubation in shaker for 8 h. The surface plasmon resonance (SPR) was observed around 420-430 nm (Fig. 2a) due to the excitation of the surface plasmon present on the outer surface of the AgNPs. The colour change from yellowish to brown is an observation method generally used for screening bacteria for AgNPs synthesis¹²⁻¹⁴. The UV-vis spectrum reveals strong absorbance between 425-430 nm signifying the formation of AgNPs. The ultraviolet-visible spectra of the cell filtrate with AgNO₃ showed a strong broad peaks at 440 nm²¹, 420 nm²² and 410-450 nm²³ indicating the presence of AgNPs.

E-dax analysis of AgNPs was confirmed the presence of silver (Fig. 2b). The morphology and size of the AgNPs were nearly spherical, rod shape and the particles were uniformly distributed (Fig. 2c and 2d). Magudapathy *et al.*²⁴ reported that AgNPs usually exhibit typical optical absorption signals at <3 keV that could be due to the SPR. Similar results were observed by Shukla *et al.*²⁵ reported that the EDX spectrum of agar-stabilized AgNPs had the strongest peaks at <3 keV and carboxymethyl cellulose (CMC) stabilizing AgNPs consisted of Ag, O, and C with percentages of 18.99, 47.54, and 33.47%, respectively²⁶.

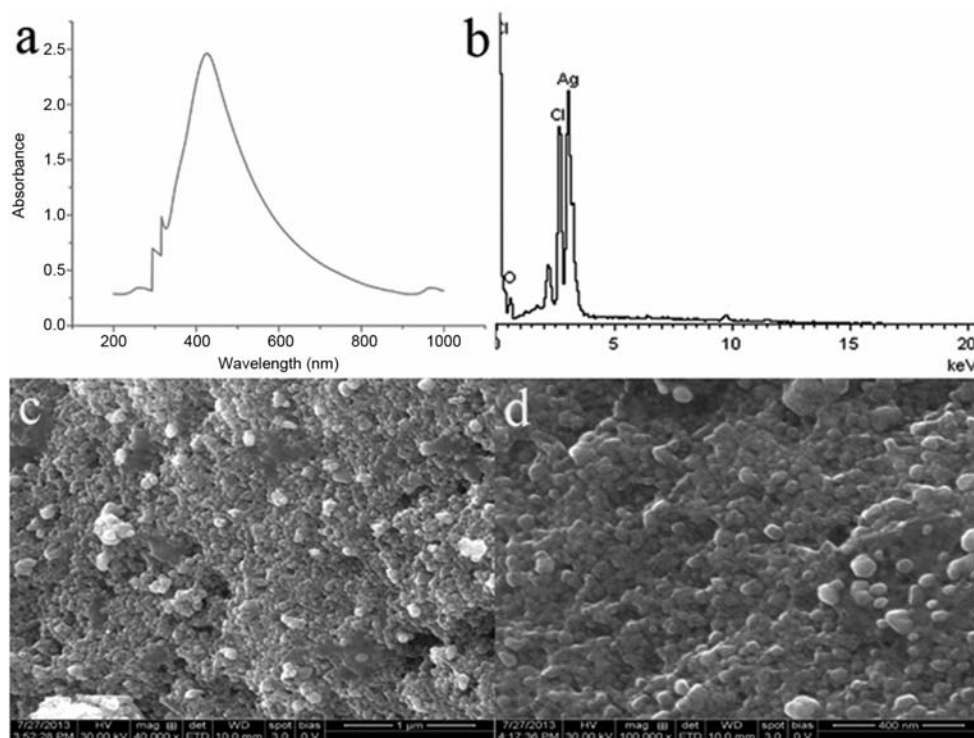


Fig. 2 — a) UV-vis spectrum of AgNPs b) E-dax spectrum of AgNPs and SEM images of AgNPs at different scale (c and d).

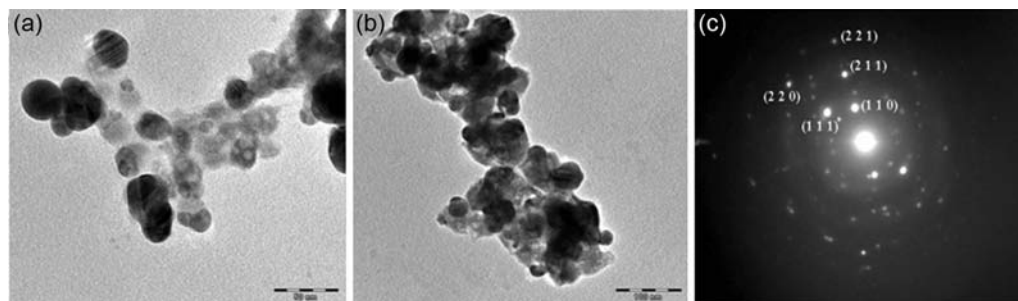


Fig. 3 — TEM micrograph (a and b) and SAED pattern of AgNPs. The AgNPs of SAED pattern (c) compared with JCPDS file no. 76-1393.

Further the size of the AgNPs are also confirmed by TEM micrograph (Fig. 3a and 3b) and SAED pattern confirms the presence of Ag crystal by exhibiting the diffraction at five different planes such as (1 1 0), (1 1 1), (2 2 0), (2 1 1) and (2 2 1). The SAED results confirmed with standard JCPDS data file No. 76 - 1393. The size of AgNPs synthesized was 50 nm and the diameter was ranged from 20-100 nm²⁷, 19 nm²⁸ and spherical, triangular, rod and hexagonal shaped structures ranging from 2 to 5 nm with an average size of 10 nm²⁹. In addition, spherical shaped AgNPs have been synthesized with an average size of 5-10 nm using polysaccharides such as soluble starch and dextran as reducing and stabilizing agents^{30,31}. The DLS graph of AgNPs showed that nanoparticles were 32-40 nm in range. The zeta potential of AgNPs measured in the ratio of 1:11 was at -16.2mV (Fig. 4b) and the stability of nanoparticles was good due to the presence of potential charges on the surfaces.

The XRD patterns of AgNPs showed diffraction peaks around 33°, which are indexed (111) of the wurtzite crystal structure of AgNP (Fig. 4a). With reference to the JCPDS data file No. 76 - 1393 concluded that the nanoparticles were crystalline in nature having cubical shape with no such impurities. The XRD spectrum of the AgNPs exhibited four intense peaks at 38.9, 44.4, 64.6 and 78.3 in the 2 theta region, corresponding to (1 1 1), (2 0 0), (2 2 0) and (3 1 1) planes of silver²⁶. These typical XRD peaks occur due to the presence of a face centered cubic (fcc) structure of the crystalline AgNPs³². AgNPs size ranges between 30-34 nm calculated using Debye-Scherrer Equations.

The FT-IR spectrum of the AgNPs revealed various characteristic peaks ranging from 3420 to 821 cm⁻¹. In the present study, FTIR spectrum of AgNPs (Fig. 4b) showed the band at 3440 cm⁻¹ corresponds to O-H stretching H-bonded alcohols and phenols. The peak found around 1634 cm⁻¹ showed a stretch for C-H bond, peak around 1082 cm⁻¹ showed the bond stretch for N-H. Therefore the synthesized nanoparticles were surrounded by proteins, metabolites and having

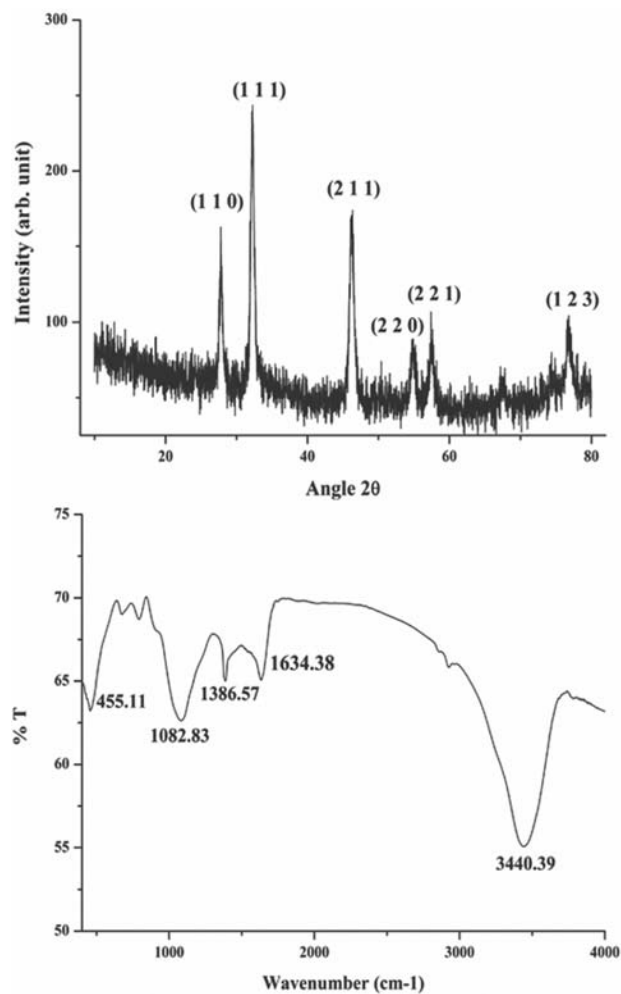


Fig. 4 — a) XRD pattern of AgNPs and b) FT-IR spectrum of AgNPs

functional groups. Moreover, the intense absorption peaks at 1783-1653 cm⁻¹ corresponds to the carbonyl (C=O) stretching frequency and carboxyl groups. The broad peaks around 1260-1040 cm⁻¹ corresponds to C-O-C and C-O stretching, and the intense peak at 995 cm⁻¹ indicating the presence of carbohydrates³³.

Vidhu and Philip² reported that the MO is an organic sulfosal dye, the high activity and specific SPR can

increase the reduction rate and reducing efficiency. The effect of different concentration of AgNPs on different concentration of MO was estimated using spectrometrically and FT-IR spectrum analysis. The degradation of MO using AgNPs were monitored at every 6 h period interval and results indicated that the increase of AgNPs concentration decreases the colour

of MO. Kumar *et al.*¹⁸ reported that the photocatalytic degradation of AgNPs increased with increase of time. Almost 96% of MO (100 $\mu\text{g/mL}$) was degraded with 200 $\mu\text{g/mL}$ concentration of AgNPs (Fig. 5), while 92, 86, 82, 79, 74, 69 and 62% of MO (200-2000 $\mu\text{g/mL}$) was degraded after treatment with 200 $\mu\text{g/mL}$ concentration of AgNPs that revealed the increase of

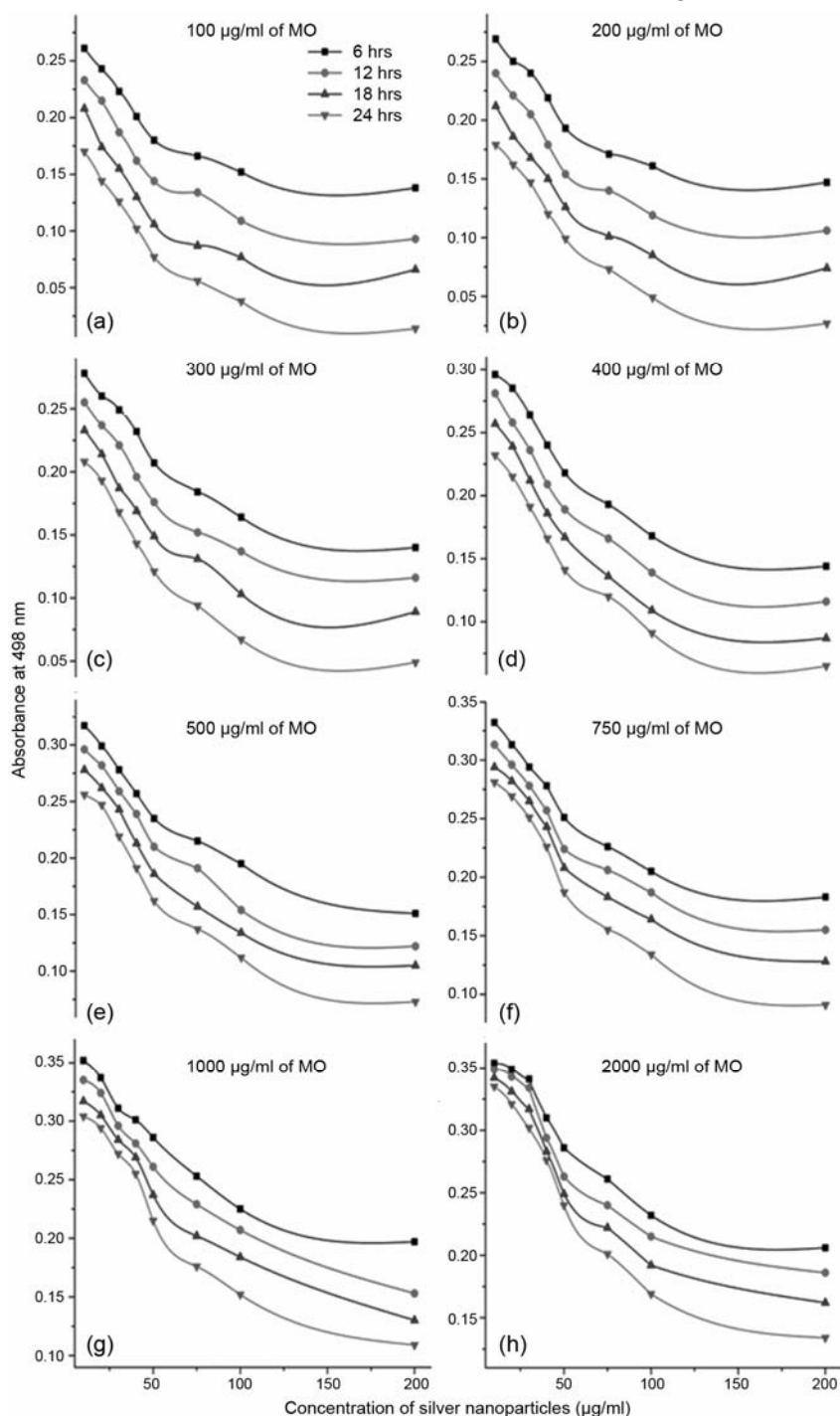


Fig. 5 — Photocatalytic degradation of 100-2000 $\mu\text{g/mL}$ concentration of MO (a-h) using AgNPs (200 $\mu\text{g/mL}$).

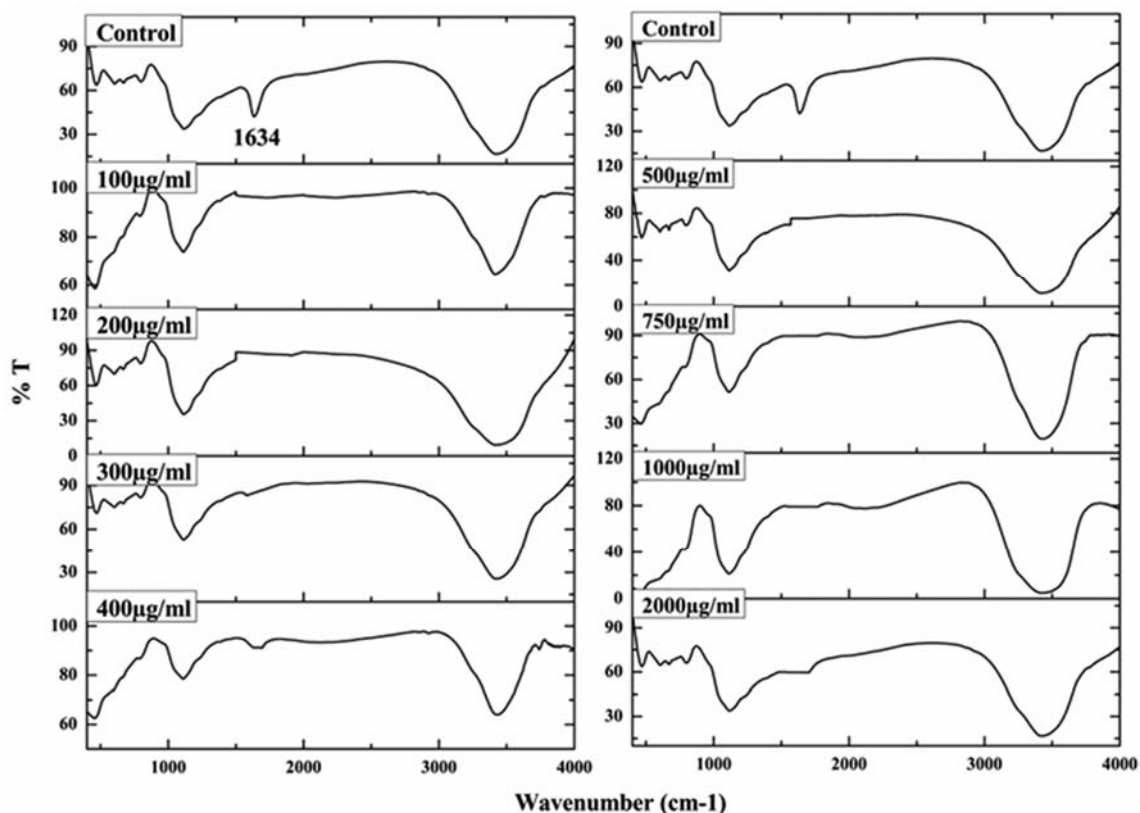


Fig. 6 — FT-IR spectrum of 200 µg/mL concentration of AgNPs treated MO (100-2000 µg/mL). Without AgNPs exposure used as control.

AgNPs concentration effectively degrades the MO. Kansal *et al.*³⁴ reported that compared to other irradiation techniques, solar light was found to be faster in decolorizing MO in the presence of metal catalyst. Moreover, the photocatalytic properties of Ag nanoparticles were excellent due to the SPR that spread the interface at metal and dielectric medium³⁵. Wang *et al.*³⁶ stated that, Ag nanoparticles are excellent, proficient and stable photocatalysts for degrading organic compounds and dyes in ambient temperature under visible light.

The FT-IR spectrum was analyzed after 24 h treatment of MO with high concentration of AgNPs (200 µg/mL). FT-IR analysis shows the AgNPs were efficiently break down the N=N bond (Fig. 1) and disperse the MO (Fig. 6). The consumption of MO by AgNPs was increased with increase in the concentration of AgNPs (Fig. 7) that suggested that the AgNPs was effectively degrade the MO. FTIR spectra of MO display a peak at 2,924.06 cm⁻¹ for asymmetric -CH₃ stretching vibrations; peaks at 1,519.78 and 1,421.71 cm⁻¹ for the C = C-H in plane C-H bend; peaks at 1,040.00, 1,007.29, and 846.66 cm⁻¹ for ring vibrations; and a peak at

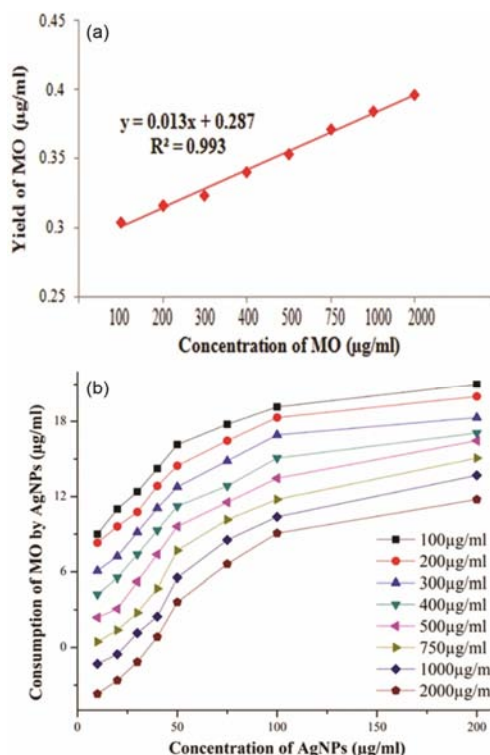


Fig. 7 — Consumption of MO by different concentration of AgNPs (b) using the standard calibration curve of MO (a)

Table 1 — Phytotoxicity evaluation of before and after treated MO with AgNPs.

Parameter	Water	MO	MO after treatment
Germination (%)	95	20	80
Shoot length (cm)	8.9±0.2	2.6±0.1	7.2±0.4
Root length (cm)	7.2±0.3	2.2±0.3	5.7±0.3
Phenols (µg/mL)	12.6445	2.2463	9.2648
Flavonoids (µg/mL)	12.9135	2.3172	9.4128

816.67 cm⁻¹ for the disubstituted benzene ring that confirms the aromatic nature of the dye³⁷. The azo peak of dye was disappeared into amines with existence of large peak at 3440.46 cm⁻¹ corresponds to amines and phenolic groups³⁸. Olukanni *et al.*³⁹ reported that the disappearance of 1049.36 cm⁻¹ and 1034.44 cm⁻¹ that corresponds to sulfonic functions.

The average value for the root length and shoot length of 10 seeds of *O. sativa* in control was obtained 8.4 ± 0.2 cm and 6.4 ± 0.3 cm respectively with 95% of germination (Table 1). Whereas the shoot length of about 0.6 ± 0.1 cm and 0.7 ± 0.3 cm for untreated dye and 7.2 ± 0.4 cm and 5.7 ± 0.3 cm for treated dye was obtained. The results indicated that the 71% and 19% of shoot length was decreased in rice grown by untreated dye and treated dye respectively with 20% and 80% of germination. The yield of phenol and flavonoids in after and before treatment was also measured using galic acid and rutin as standards. The results showed that the amount of phenols and flavonoids were significantly high in plant grown using treated dye than the untreated dye, that confirms the dye treated with AgNPs has less toxicity. Shah *et al.*²⁰ and Nouren and Bhatti⁴⁰ reported that the treated dye has less toxicity than the untreated and enhances the growth of plants.

Conclusion

Dyes are one of the major pollutants threaten to our environment and also very harmful to all the species on earth and it will destroy the ecosystem. The present demonstrate that the degradation of such harmful dye MO using AgNPs and the treated dye evaluated its phytotoxicity analysis. The development of such particles may be considered a breakthrough in the field for the efficient clean up of the dyes on large scale process since nanoparticles are easy to synthesize on large scale and cost effective.

Acknowledgement

The authors acknowledge the authorities of Bharathidasan University for providing the facilities to carry out this work.

References

- Puvaneswari N, Muthukrishnan J & Gunasekaran P, *Indian J Exp Biol*, 44 (2006) 618.
- Vidhu V K & Philip D, *Micro*, 56 (2014) 54.
- Jain K, Shah V, Chapla D & Madamwar D, *J Hazard Mater*, 213 (2012) 378.
- Liu G, Zhou J, Wang J, Wang X, Jin R & Lu H, *Appl Microbiol Biotechnol*, 91 (2011) 417.
- Ali H, *Water Air Soil Pollut*, 213 (2010) 251.
- Wang H Q, Li G H, Jia L C, Wang G Z & Tang C J, *J Phys Chem C*, 112 (2008) 11738.
- Nishio J, Tokumura M, Znad H T & Kawase Y, *J Hazard Mater*, 138 (2006) 106.
- Kalyani D C, Telke A A, Dhanve R S & Jadhav J P, *J Hazard Mater*, 163 (2009) 735.
- Mohamed R M, Mkhaliid I A, Baieissa E S & Al Rayyani M A, *J Nanotechnol*, (2012) 329082.
- Shahverdi A R, Minaeian S, Shahverdi H R, Jamalifar H & Nohi A A, *Proc Biochem*, 42 (2007) 919.
- Sankar, R, Karthik A, Prabu A, Karthik S, Shivashangari K S & Ravikumar V, *Colloids Surf B*, 108 (2013) 80.
- Kalimuthu K, Babu R S, Venkataraman D, Bilal M & Gurunathan S, *Colloid Surf B*, 65 (2008) 150.
- Saravanan M, Vemu A K & Barik S K, *Colloids Surf B*, 88 (2011) 325.
- Shivaji S, Madhu S & Singh S, *Proc Biochem*, 49 (2011) 830.
- Ramalingam V, Rajaram R, Premkumar C, Santhanam P, Dhinesh P, Vinothkumar S & Kaleshkumar K, *J Basic Microbiol*, 54 (9) (2014) 928.
- Cruickshank R, Duguid J P, Marmion B P & Svvain R H A, *The Practice of Medical Microbiology*, 12th Edn, 2 (1975) 307.
- Chakravorty S, Danica H, Burday M, Connell N & Alland D, *J Microbiol Methods*, 69 (2007) 330.
- Kumar P, Govindaraju M, Senthamilselvi S & Premkumar K, *Colloid Surf B*, 103 (2013) 658.
- Chen K C, Wu J Y, Liou D J & Hwang S C, *J Biotechnol*, 101 (1) (2003) 57.
- Shah P D, Dave S R & Rao M S, *Int Biodeter Biodegr*, 69 (2012) 41.
- Li G, He D, Qian Y, Guan B, Gao S, Cui Y, Yokoyama K & Wang L, *Int J Mol Sci*, 13 (2012) 466.
- Gurunathan S, Kalishwaralal K, Vaidyanathan R, Deepak V, Pandian S R K, Muniyandi J, Hariharan N & Eom S H, *Colloid Surf B*, 74 (2009) 328.
- Das V L, Thomas R, Varghese R T, Soniya E V, Mathew J & Radhakrishnan E K, *3 Biotech*, 4 (2012) 121.
- Magudapatty G, Gangopaghyayrans P, Panigrahi B K, Nair K G M & Dhara S, *Physica B Cond Mat*, 299 (2001) 142.
- Shukla M K, Singh R P, Reddy C R K & Jha B, *Bioresour Technol*, 107 (2012) 295.
- Hebeish A, Hashem M, Abd El-Hady M M & Sharaf S, *Carbohydr Poly*, 92 (2013) 407.
- Jeevan P, Ramya K & Edith Rena A, *Ind J Biotech*, 11 (2012) 72.
- El Batal A I, Amin M A, Shehata M M K & Hallol M M A, *World Appl Sci J*, 22 (1) (2013) 1.
- Kanmani P & Lim S T, *Proc Biochem*, 48 (2013) 1099.
- Mohanty S, Mishra S, Jena P, Jacob B, Sarkar B & Sonawane A, *Nanomed Nanotechnol Biol Med*, 8 (2012) 916.

- 31 Bankura K P, Maity D, Mollick M M R, Mondal D, Bhowmick B, Bain M K, Chakraborty A, Sarkar J, Acharya K & Chattopadhyay D, *Carbohydr Poly*, 89 (2012) 1159.
- 32 Pandey S, Goswami G K & Nanda K K, *Int J Biol Macromol*, 51 (2012) 583.
- 33 Kanmani P, Satishkumar R, Yuvaraj N, Paari K A, Pattukumar V & Arul V, *Crit Rev Food Sci Nut*, 53 (2012) 641.
- 34 Kansal S K, Singh M & Sud D, *J Hazard Mater*, 153 (2008) 412.
- 35 Garcia M A, *J Phys D Appl Phys*, 44 (2011) 283001.
- 36 Wang P, Huang B, Qin X, Zhang X, Dai Y, Wei J, Whangbo M H, *Angewandte Chemie*, 47 (41) (2008) 7931.
- 37 Kalyani D C, Phugare S S, Shedbalkar U U & Jadhav J P, *Ann Microbiol*, 61 (2010) 483.
- 38 Shekhar B J, Swapnil S P, Pratibha S P & Jyoti P J, *Int Biodeter Biodegr*, 65 (2011) 733.
- 39 Olukanni O D, Osuntoki A A, Kalyani D C, Gbenle G O & Govindwar S P, *J Hazard Mater*, 184 (2010) 290.
- 40 Nouren S & Bhatti H N, *Biochem Eng J*, 95 (2015) 9.